Accelerating diffusion tensor imaging using multi-reference image constrained reconstruction

L. J. Healy[1], O. Abdullah[1], and E. W. Hsu[1]

[1]Bioengineering, University of Utah, Salt Lake City, UT, United States

Introduction: MR diffusion tensor imaging (DTI) [1] has been increasingly used to quantitatively characterize the microstructure of ordered tissues such as the brain white matter. However, practical applications of DTI are hampered by the low SNR, long acquisition times, and low spatial resolution. Since in DTI essentially the same image (except for diffusion encoding) is acquired repeatedly, reduced encoding and single-reference constrained reconstruction have been shown to improve the DTI scan efficiency [2]. Separately, more accurate capturing of the image contrast has been achieved by constrained reconstruction using two reference images [3]. The goals of the current study are to extend multi-reference constrained reconstruction to DTI, and evaluate whether the methodology can further improve the scan time efficiency of DTI.

Methods: A fixed feline brain specimen was obtained from an unrelated study. DTI experiments were conducted on a Bruker Biospec 7.0 T scanner using standard 3D spin echo sequence (500/17 ms TR/TE, 128 x 128 x 64 matrix size at 450 μm isotropic resolution). Two redundant "gold standard" DTI datasets were obtained, each including a b0 image and 15 diffusion-weighted (nominal b value of 781 s/mm^2) encoded in a set of 12 optimized gradient directions [4] plus laboratory x, y, and z axes. Three reduced sampling and constrained reconstruction DTI schemes were analyzed. First, reduced encoding imaging via generalized series reconstruction (RIGR) [5] was used to reconstruct diffusion-weighted images from the central 1/4 (1/2 in each phase and slice axes) of their k-space with the full-resolution b0 image as the single reference. Second, the central 1/16 k-space was used to reconstruct diffusion-weighted images using full-resolution b0 and diffusion images encoded in the x, y, and z axes. Extending the concept of two-reference RIGR [3], the reference image for the diffusion contrast was generated by the difference between b0 and quadratic superposition (based on directional cosines) of the x, y, and z-weighted images. Third, the full-resolution b0 and 4 diffusion images were initially used to solve for the simplified (or axisymmetric) tensor [6]. Subsequently, the diffusion image predicted by the solution for the particular direction was used as RIGR reference for reconstructing the central 1/16 k-space of the same direction. To provide a basis for comparison, a minimum DTI experiment was simulated from full-resolution b0 and diffusion images encoded in randomly selected 6 (unoptimized) of the 15 encoding directions. DTI results from each scheme were evaluated by comparing the fractional anisotropy (FA) values and primary eigenvector (EV1) to those obtained from the redundant gold-standard dataset. Lastly, to a first approximation, the effective acceleration factor (EAF, or the factor of scan time savings for achieving the same accuracy) for each FA and EV1 measurements of each scheme was computed according to,

$$EAF = (\Delta_{GS-GS} / \Delta_{scheme-GS})^2 / (T_{GS} / T_{scheme}),$$

where Δ is the FA difference or EV1 angular difference, and T is the acquisition time.

Results and Discussion: Representative FA maps obtained for the minimum, RIGR, gradient-weighted (GW) RIGR, model-based (MB) RIGR and gold standard DTI experiments are shown in Figure 1. Qualitatively, the minimum experiment yielded an FA map that is similar to the gold standard but compromised by noise (and "holes" created by failed tensor fitting). Conspicuous blurring is observed for RIGR, but is improved in GW-RIGR. In contrast, MB-RIGR produced the most accurate FA map. The differences of FA and EV1 of each DTI scheme with respect to the gold standard are tabulated in Table 1, which supports the dramatic accuracy improvement observed for MB-RIGR. The EAFs computed for FA and EV1 are separately listed in Table 2, which compare the relative performance of DTI measurement accuracy on a normalized basis. (An EAF greater than unity means that a measurement accuracy equal to that of the gold standard can be achieved in a scan time shortened by the same factor.) Both EAFs for the minimum DTI experiment are less than unity, which likely reflects its unoptimized diffusion encoding directions. For RIGR, the EV1 EAF is greater than unity, which is consistent with the finding of a previous reduced encoding DTI study [2]. Surprisingly, RIGR does not improve the EAF for the FA, and neither does GW-RIGR for both FA and EV1. Lastly, markedly improved EAFs (i.e., greater than 1) are obtained for MB-RIGR for both FA and EV1, indicating that MB-RIGR is a viable technique to accelerate DTI acquisition. Although the difference in the two EAFs needs further investigation, even higher achievable EAFs are expected when a larger number of diffusion encoding directions (e.g., in high angular resolution diffusion imaging) are employed.

	Minimum	RIGR	GW-RIGR	MB-RIGR
Scan Time	7	4 3/4	4 3/4	5 11/16
Δ FA	0.10 ± 0.14	0.10 ± 0.08	0.10 ± 0.08	0.07 ± 0.06
Δ EV1	8.1 ± 8.5°	7.5 ± 8.2°	9.1 ± 9.4°	5.6 ± 5.7°

Table 1: The FA difference and (EV1) angular difference (mean ± standard deviation) averaged over the white matter (N = 10000 points)

	Minimum	RIGR	GW-RIGR	MB-RIGR
EAF FA	0.486	0.720	0.778	1.400
EAF EV1	0.872	1.517	1.020	2.235

Table 2: The equivalent acceleration factors (EAF) for FA and EV1

Conclusions: The accuracy and efficiency of selected reduced encoding and constrained reconstruction schemes for DTI were examined. Results indicate that, despite of using multiple full-resolution images, RIGR combined with using model-based estimated images as references can be used to improve the acquisition efficiency of DTI beyond what was previously achieved using single-reference RIGR.

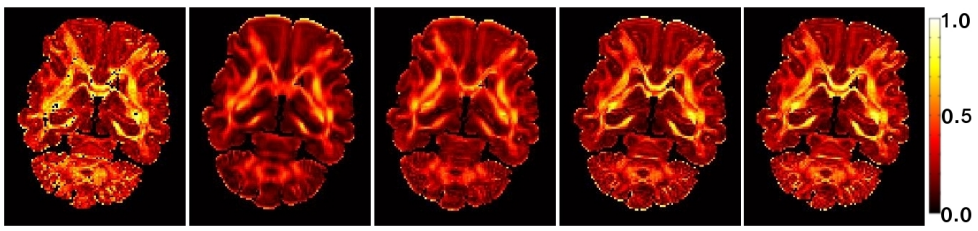

Figure 1: FA maps for the minimum, RIGR, GW-RIGR, MB-RIGR, and gold standard from left to right

References:

1. Basser, P.J., et al. J Magn Reson B, 1994. **103**(3): p. 247-54. **2.** Hsu, E.W., et al. J Cardiovasc Magn Reson, 2001. **3**(4): p. 339-47. **3.** Hanson, J.M., et al. Magn Reson Med, 1996. **36**(1): p. 172-5. **4.** Papadakis, N.G., et al. J Magn Reson, 1999. **137**(1): p. 67-82. **5.** Liang, Z.P., et al. IEEE Trans Med Imaging, 1994. **13**(4): p. 677-86. **6.** Hsu, E.W., et al. Magn Reson Med, 1995. **34**(2): p. 194-200.